

Observations of a Rain-Formed Mixed Layer

JAMES F. PRICE

Graduate School of Oceanography, University of Rhode Island, Kingston, 02881

10 March 1978 and 23 October 1978

ABSTRACT

The structure and dynamics of a rain-formed mixed layer (ML) are studied using hourly STD and profiling current meter casts. Because the fluid beneath the rain-formed ML was vertically homogeneous, the ML buoyancy g' and horizontal velocity difference δV were easily observable as the ML depth h increased by entrainment from 7 to 18 m in a period of 8 h. The overall Richardson number of the mixed layer $g'(h + d/2)/\delta V^2 \approx 0.7$ during that period, where d is the thickness of the transition layer at the base of the ML. The entrainment rate was consistent with that of a laboratory surface half-jet (Ellison and Turner, 1959).

The transition layer thickness was an appreciable fraction of the ML thickness, roughly $d \approx h/3$. The density profile through the transition layer was linear and symmetric, and the overall Richardson number of the transition layer $g'd/\delta V^2 \approx 1/4$.

1. Introduction

A rain-formed mixed layer (ML) was observed during a field study conducted in 1972 on the west Florida continental shelf. The gross structure and dynamics of that ML are examined here using STD and profiling current meter casts (PCM) (Curtin, 1974) made at hourly intervals from an anchored ship. [See Ostapoff *et al.* (1973) and Miller (1976) for previous studies of the rainfall effect on the upper ocean. See Price *et al.* (1978) for a discussion of the complete data set from which these data were taken.]

Approximately 6 cm of rain fell in <2 h as a weak cold front passed over the experimental site from 0500 to 1100 LT 13 June (Fig. 1a). The time and dura-

tion of the rainfall are not known precisely and the magnitude is known only from a salinity budget. The rainfall represented a large, nearly impulsive buoyancy flux (equivalent to 500 cal cm^{-2}) which caused the formation of a new, shallow ML (Fig. 1b). The rain-formed ML immediately began to deepen by entrainment and within 20 h had merged with a relic ML 25 m thick formed two days earlier. While the rain-formed ML deepened, the wind stress was roughly constant in magnitude and direction and there was no significant air-sea buoyancy exchange. Hence, this is a relatively simple example of wind-driven ML deepening.

The dynamically important density and horizontal velocity differences across the base of the rain-

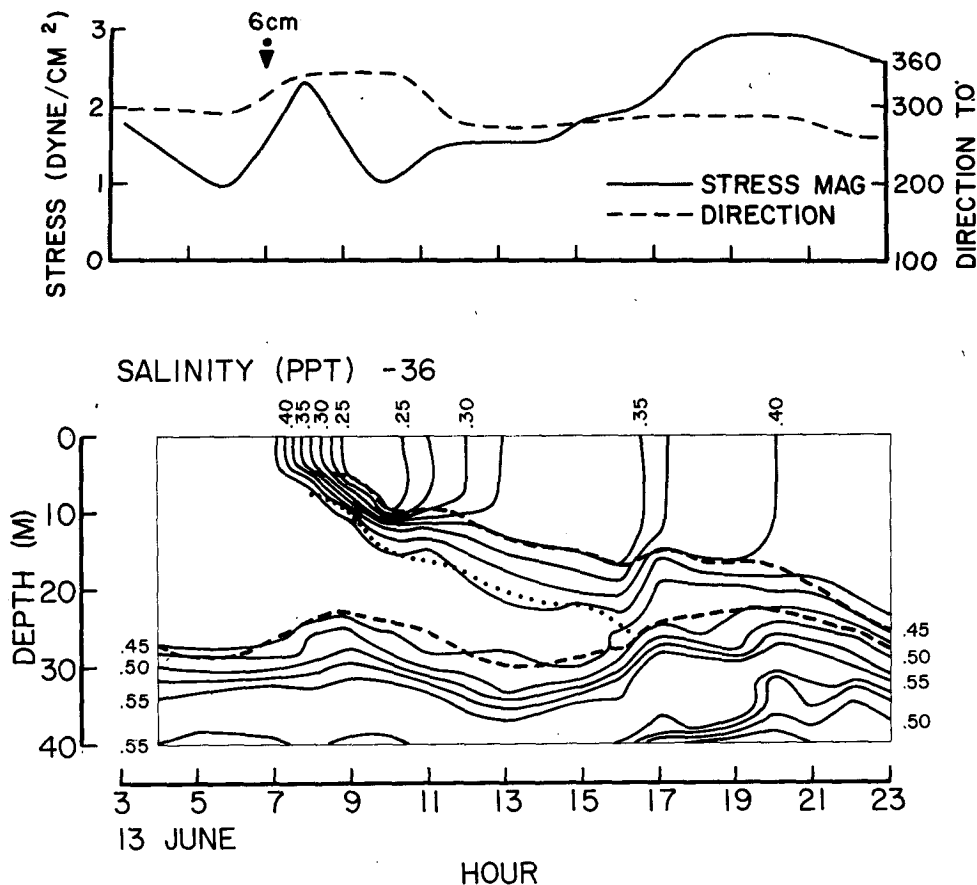


FIG. 1. (a) Wind stress computed from hourly shipboard observations of wind velocity as $\tau = \rho_a C_d |U|U$ where ρ_a is the density of air, $C_d = 1.5 \times 10^{-3}$ is the drag coefficient and U the observed wind. Rainfall is shown at 0700 LT. (b) Time-depth contour of salinity. Data matrix had $\Delta z = 2$ m and $\Delta t = 1$ h. The relic ML depth is shown as a dashed line, the base of the transition layer is shown as a dotted line, and the base of the rain-formed ML is shown as a dashed line.

formed ML were well-defined and easily observable because the fluid beneath the ML was within a relic ML and was vertically homogeneous. Therefore, it is possible to compute the overall Richardson numbers which arise in parameterizations of ML deepening and compare this oceanic case directly with laboratory models.

2. Description of the mixed layer and interior

Salinity profiles (equivalent to density profiles) through the upper 25 m showed three distinct layers; a nearly homogeneous ML of thickness h , a transition layer of thickness d and an interior which was homogeneous down to the depth of the relic ML (Fig. 2). Rainfall was occurring while profile 1 was being taken and had stopped by the time of profile 2. The total ML salinity, equal to the area to the right of the profile as plotted in Fig. 2, fluctuated $\pm 20\%$ about an average value corresponding to 6 cm of rainfall.

Rainfall caused a pronounced depression of sea surface salinity. The maximum depression was 0.25‰ immediately after the cessation of rainfall (profile 2) when the ML was 7 m thick. Sea surface salinity remained depressed approximately 0.07‰ after the rain-formed ML had completely merged with the relic ML. Elliott (1974) found little evidence of a sea surface salinity response to rainfall in BOMEX data, apparently because the rainfall signature was smaller than the fluctuation due to horizontal advection. In this case the fluctuation of sea surface salinity in the absence of rainfall was $\pm 0.02\%$.

The approximate conservation of total ML salinity indicates that the increase in ML salinity following the rainfall was due to entrainment of relatively saline water from the interior. The ML remained remarkably vertically homogeneous while this mixing process occurred; there was no consistently observable salinity gradient within the ML until the time of profile 7 when the gradient was $\sim 0.01\%$.

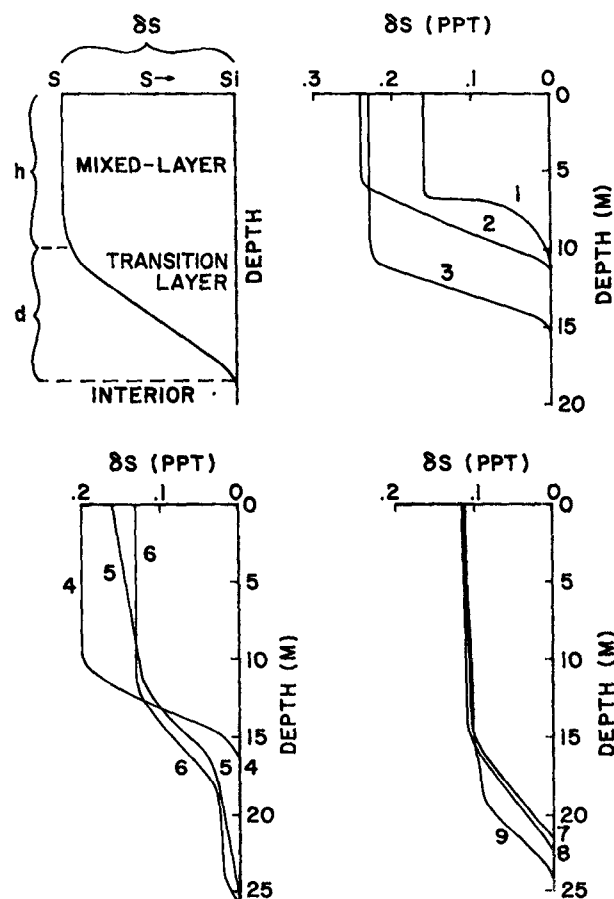


FIG. 2. STD salinity profiles made at 1 h intervals beginning at 0730 LT. The profiles are drawn with the interior salinity as the common origin. The original analog traces exhibited a rich, highly variable structure on scales of 1 m or less which has been smoothed out of these profiles.

$(10 \text{ m})^{-1}$. This implies a large vertical diffusivity within the ML ($\geq 500 \text{ cm}^2 \text{ s}^{-1}$).

Salinity in the interior fluctuated randomly $\pm 0.02\text{‰}$ about an average value of 36.47‰ (ex-

cepting profile 5). The relic ML depth appeared to closely follow the motion of the underlying isohalines (Fig. 1b). These observations indicate that the interior was passive while it was overlain and insulated from direct wind-forcing by the rain-formed ML.

3. The transition layer

The density profile through the transition layer was approximately symmetric and linear in every profile except 1 which was made while rainfall was still occurring (Fig. 2). Symmetric transition layers occur in grid-stirred entrainment experiments in which upper and lower layers are stirred equally (Crapper and Linden, 1974) or when a shear exists across the transition layer (Moore and Long, 1971; Thorpe, 1971). Entrainment was entirely asymmetric in this case, suggesting that turbulence in the ML probably did not control the transition layer structure as it does in grid-stirred experiments. This may also be inferred from the thickness of the transition layer; the energy required to lift a unit mass of fluid from the interior through the transition layer is $g'd/2 \approx 50 \text{ cm}^2/\text{s}^2$, where $g' = g\delta\rho/\rho$ is the buoyancy of the ML and g is the acceleration of gravity. An eddy thus needed a vertical velocity of at least 7 cm s^{-1} to penetrate through the transition layer. This is greatly in excess of likely values (Arsenyev *et al.*, 1976) and indicates that turbulent motions within the ML penetrated only a relatively thin upper edge of the transition layer.

The linearity and symmetry of the transition layer density profile suggest that the thickness and structure of the layer may have been controlled by the mean velocity shear across the layer (Turner, 1973, p. 186). To examine this we define an overall Richardson number of the transition layer,

$$R_t = \frac{g'd}{\delta V^2},$$

TABLE 1. Mixed-layer variables.

STD profile no.	Time 13 June (local)	δS (‰)	δT (°C)	h (m)	d (m)	δV_z (cm s ⁻¹)	δV_0 (cm s ⁻¹)
1	0729	0.16 ± 0.01	0.04 ± 0.01	$7 \pm \frac{1}{2}^a$	2 ± 1	6.5	
2	0830	0.24	0.07	$7 \pm \frac{1}{2}$	$4 \pm \frac{1}{2}$	13.7	
3	0926	0.23	0.08	11 ± 1	$4 \pm \frac{1}{2}$	15.3	
4	1028	0.20	0.10	10 ± 2	$5 \pm \frac{1}{2}$	15.9	
5	1130	0.16	0.05	12 ± 2	6 ± 1	16.5	15.4 ± 4.0
6	1233	0.13	0.02	12 ± 1	6 ± 1	15.8	14.5
7	1330	0.11	0.03	15 ± 1	$6 \pm \frac{1}{2}$	14.4	13.6
8	1432	0.11	0.02	$15 \pm \frac{1}{2}$	$7 \pm \frac{1}{2}$	13.6	12.8
9	1533	0.10	0.02	18 ± 1	6 ± 1	14.0	12.3

^a The uncertainties in h and d result from displacements of the transition layer between up and down going STD profiles and from departures from the assumed model profile.

^b No velocity observations are available during this period due to instrument malfunction.

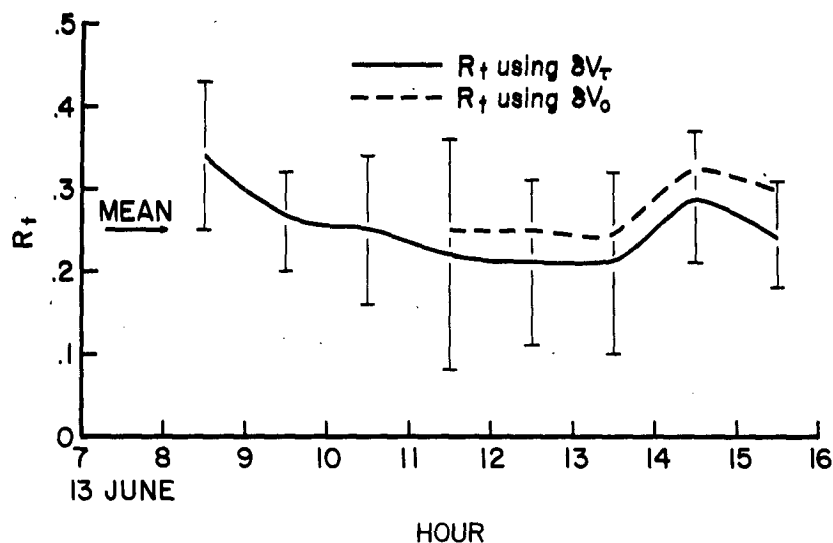


FIG. 3. The bulk Richardson number of the transition layer, $R_t = g'd/\delta V^2$, computed from the estimates of d , δT , δS and δV given in Table 1.

where δV is the magnitude of the horizontal velocity difference across the transition layer. It was noted above that the density profile through the layer was linear. If the velocity profile was similar (this cannot be confirmed with the PCM observations) then R_t is equal to the gradient Richardson Ri number within the transition layer.

The temperature and salinity differences across the transition layer, δT and δS , and the layer thickness were read directly from analog STD traces (Table 1). ML buoyancy was computed as $g' = g(-3.6 \times 10^{-4} \delta T + 7.0 \times 10^{-4} \delta S)/\rho$. The velocity difference was computed from direct PCM velocity observations (δV_o) when they were available and

from observed wind stress and ML depth (δV_τ) using the one-dimensional momentum conservation equation

$$\frac{d\delta V}{dt} = \frac{\tau}{h\rho} + \frac{dh}{dt} \frac{\delta V}{h} - f \times \delta V, \quad (1)$$

where d/dt is an ordinary time derivative, τ the wind stress and f the Coriolis parameter times the vertical unit vector. In deriving (1) it was assumed that all wind stress was absorbed within the ML. The initial condition was $\delta V = 0$ at 0700, the approximate time that the ML was formed. When both computed and observed estimates of δV are available they are very similar. Most of the contribution to δV was

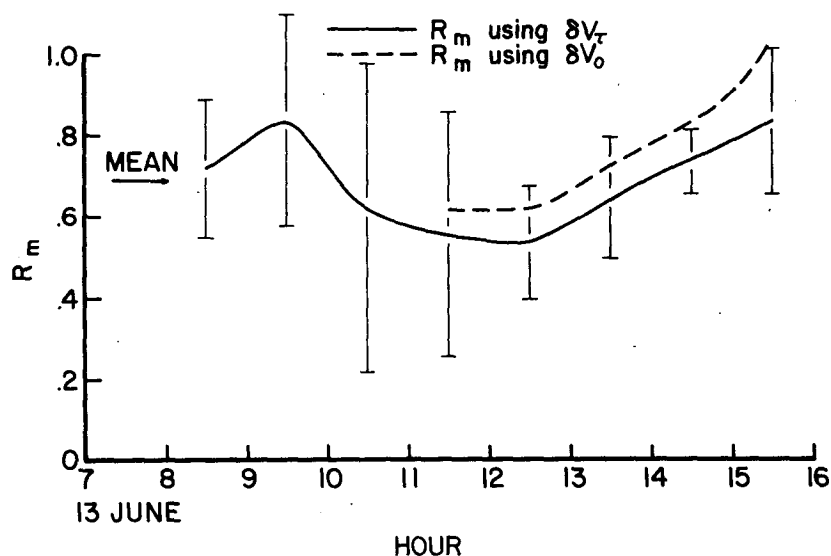


FIG. 4. The bulk Richardson number of the mixed layer, $R_m = B/\delta V^2$, computed from the estimates of d , h , δT , δS and δV given in Table 1.

due to a change in direction of $\sim 40^\circ$ across the transition layer. The difference in velocity magnitude across the transition layer was only 2–3 cm s^{-1} .

The average value of R_t over the period 0830 to 1530 LT was 0.26 (Fig. 3). This mean value is within the error bound of each estimate and there is no suggestion of a trend developing as the ML deepens. Hence, it appears that the transition layer was in an equilibrium state set by the familiar stratified shear flow stability limit, $R_t \sim Ri = 1/4$. The transition layer was driven toward instability by ML deepening which had a characteristic time scale $[d(\ln h)/dt]^{-1} \approx 5$ h. Instability was (apparently) relieved by the relatively fast (0(100)s; Thorpe, 1973) growth and collapse of shear flow instabilities. Csanady (1974) and Mahrt and Lenschow (1976) have developed ML models which include a transition layer very similar to the one observed here.

4. Deepening of the rain-formed mixed layer

Wind-driven ML deepening must be parameterized in any operationally useful upper ocean model. Price *et al.* (1978) tested several plausible parameterizations by simulating observed, time-dependent deepening events. A successful parameterization had the form

$$\frac{dh}{dt} / \delta V = E(R_m),$$

where

$$R_m = \frac{B}{\delta V^2}$$

is a bulk Richardson number of the ML and $B = g'(h + d/2)$ is the total ML buoyancy. $E(R_m)$ was found to decrease sharply as R_m exceeded ~ 0.6 . A ML which follows such an entrainment law would have $R_m \approx 0.6$, while it was deepening strongly ($E \geq 10^{-3}$); the time-average R_m of the rain-formed ML for the period 0830 to 1530 LT was 0.70 ± 0.15 (one standard deviation) (Fig. 4). [A ML which is not deepening or deepening only very weakly ($E \leq 10^{-4}$) could assume larger values of R_m and not be inconsistent with the Price *et al.* (1978) result.]

It is not possible to determine the functional form of E by plotting the hourly estimates of E vs R_m because the uncertainty in the hourly estimates is large compared with any trend R_m and dh/dt may have. A single stable estimate of E and R_m may be computed by averaging over the period 0830 to 1530 LT. The rate of ML deepening was roughly constant during that period and is estimated to be $dh/dt \approx 13 \pm 1$ m (7 h^{-1}) $= 5.1 \pm 0.4 \times 10^{-2} \text{ cm s}^{-1}$. The velocity difference δV was also roughly constant at $15 \pm 1 \text{ cm s}^{-1}$, giving a normalized

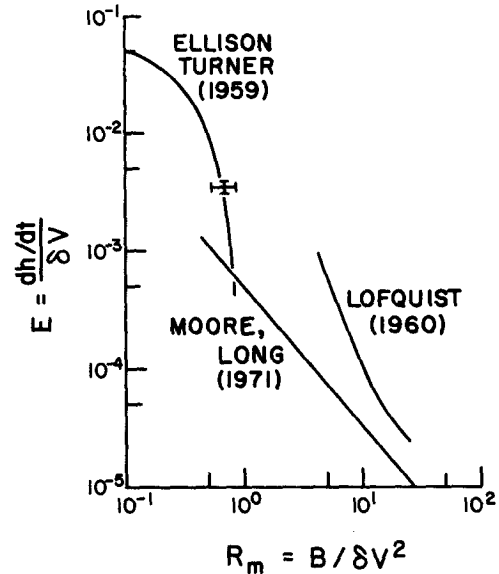


FIG. 5. $E(R_m)$ observed in three laboratory experiments and the single data point computed for the rain-formed ML. The length scale of the bulk Richardson number used by Moore and Long (1971) was the total depth of the tank D ; the data are replotted here using $D/2$. The length scale used by Lofquist (1960) was the hydraulic radius; the data are replotted here using $h + d/2$.

entrainment rate $E = 3.4 \pm 0.3 \times 10^{-3}$. The single data point from the rain-formed ML is consistent with the Ellison and Turner (1959) result for a surface half-jet (Fig. 5). It is not consistent with the entrainment law of the Moore and Long (1971) experiment (this may not be significant because Moore and Long used the depth of their tank as the length scale in their bulk Richardson number) and is outside the range of the Lofquist (1960) experiment.

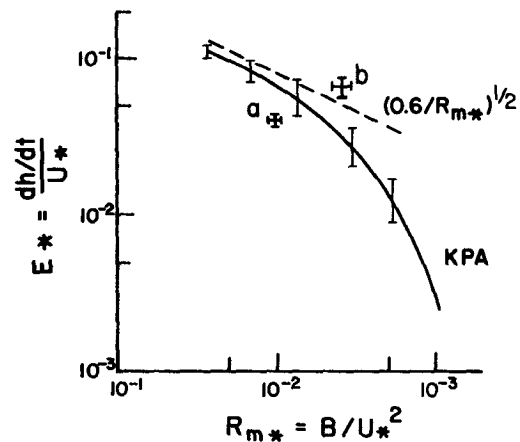


FIG. 6. The experimental result $E_*(R_m^*)$ of the KPA experiment. Points a and b are computed for the rain-formed ML using the observed wind stress and the effective stress respectively. The dashed line is the entrainment rate predicted by Price (1978), $E_* = R_m^{1/2} R_m^{*-1/2}$, where $R_m = 0.6$.

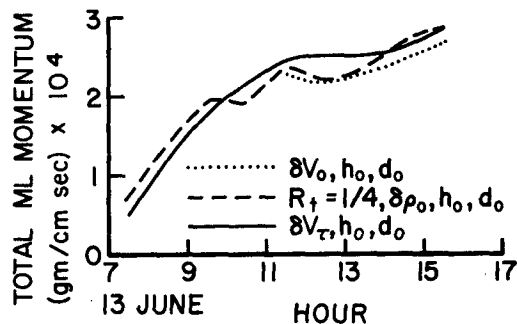


FIG. 7. Total ML momentum, $M = \delta V(h + d/2)\rho$. δV has been computed from direct observations (dotted line), by using $R_t = 1/4$ to compute δV from observations of $\delta\rho$ and d (dashed line), and from (1) (solid line).

An alternative parameterization of ML deepening is suggested by the experiment of Kantha *et al.* (1977, hereafter KPA). KPA modeled quasi-steady wind-driven deepening by applying a constant stress τ to the surface of a two-layer fluid. The observed deepening rate was nondimensionalized with the friction velocity $U_* = (\tau/\rho)^{1/2}$ and given as

$$\frac{dh}{dt} / U_* = E_*(R_m^*),$$

where

$$R_m^* = \frac{B}{U_*^2}.$$

In this case the wind stress was nearly constant at 1.5 ± 0.2 dyn cm⁻² (Fig. 1a), hence $E_* = 4.1 \pm 0.5 \times 10^{-2}$, and $R_m = 95 \pm 8$ which is labeled a in Fig. 6. Price (1978) argued that E_* for a quasi-steady two-layer case should follow the simple result

$$E_* = R_m^{1/2} R_m^{*-1/2}, \quad (2)$$

where $R_m \approx 0.6$. For application of (2) to this case the relevant stress is the component parallel to δV , called the effective stress, which is computed from the rate of change of total ML momentum, $M = \delta V(h + d/2)\rho$ (Fig. 7).¹ During the period 0830 to 1530 LT the increase in M is estimated as $1.4 \pm 0.2 \times 10^4$ g cm⁻¹ s⁻¹ implying an effective stress of 0.55 ± 0.07 dyn cm⁻². Using the effective stress, $E_* = 6.7 \pm 1.0 \times 10^{-2}$, and $R_m^* = 260 \pm 35$ which is labeled b.

Point a is a factor 1.7 below the KPA curve;

¹ Caldwell and Elliot (1971) have noted that rainfall carries horizontal momentum which they estimated as $\tau = 0.85 \rho U R$, where U is the wind velocity at 10 m height and R is the rainfall rate. In this case, $U \approx 8$ m s⁻¹ and the total rainfall was ~ 6 cm, hence, the contribution to M due to rainfall would be $\sim 0.4 \times 10^4$ g cm⁻¹ s⁻¹. This is more than enough to account for the initial discrepancy between M computed from δV , and from $R_t = 1/4$, but is small compared to the net contribution from wind stress.

point b is a factor 1.3 above the prediction of (2). Given the error estimates, neither point is grossly inconsistent and we cannot conclude whether the stress or the effective stress is most appropriate for U_* scaling of entrainment observed here.

A general conclusion is that laboratory models do appear useful for studying wind-driven deepening. This is not obvious *a priori*; Reynolds number similarity, surface waves and rotation are missing from the laboratory models and may or may not play a crucial role in oceanic wind-driven deepening.

5. Remarks

The observed structure of this rather shallow ($h < 20$ m) rain-formed ML supports the conventional model of the ML reviewed by Niiler and Kraus (1977). The interior was passive as usually assumed. The ML was thoroughly stirred and remained remarkably homogeneous with respect to density even while rapidly deepening. The transition layer at the base of the ML had an appreciable thickness set by the familiar shear flow stability criterion.

The observed dynamics (entrainment rate) of this rain-formed ML is consistent with at least one laboratory experiment (Ellison and Turner, 1959); the Niiler and Kraus (1977) model can be made consistent with these observations given the freedom to specify several model parameters. These are encouraging results, but they do not mean that we understand ML dynamics in any fundamental way. For example, these observations suggest that an important role of mean velocity shear is to maintain a relatively thick transition layer. Mean velocity shear *alone* would only be expected to thicken the transition layer symmetrically (Thorpe, 1971). Net downward penetration occurs because the transition layer steadily loses mass to the turbulent ML but not to the interior. Does turbulence within the ML actively gouge fluid out of the transition layer? Or does it merely sweep away fluid which is ejected during the collapse of instability events? Detailed knowledge of that local process may be a key to understanding ML dynamics.

Acknowledgments. This research was begun at the University of Miami, Rosenstiel School of Marine and Atmospheric Science, under Grant GA-34009 from the National Science Foundation. Dr. C. N. K. Mooers is thanked for his constant support and encouragement and Mr. T. B. Curtin is thanked for generously providing the PCM observations.

REFERENCES

- Arsenyev, S. A., S. V. Dobroklonskiy, R. M. Mamedov and N. K. Shelkovnikov, 1976: Direct measurements of small-scale marine turbulence characteristics from a

- stationary platform in the open sea. *Izv. Atmos. Oceanic Phys.*, 11, 845-850.
- Caldwell, D. R., and W. P. Elliott, 1971: Surface stresses produced by rainfall. *J. Phys. Oceanogr.*, 2, 145-148.
- Csanady, G. T., 1974: Equilibrium theory of the planetary boundary layer with an inversion lid. *Bound.-Layer Meteor.*, 6, 63-80.
- Crapper, P. F., and P. F. Linden, 1974: The structure of turbulent density interfaces. *J. Fluid Mech.*, 78, 155-175.
- Curtin, T. B., 1974: A shipboard self-contained profiling system. *Exposure*, 2, 5-7.
- Elliott, G. W., 1974: Precipitation signatures in sea-surface-layer conditions during BOMEX. *J. Phys. Oceanogr.*, 4, 498-501.
- Ellison, T. H., and J. S. Turner, 1959: Turbulent entrainment in stratified flows. *J. Fluid Mech.*, 6, 423-448.
- Kantha, L. H., O. M. Philips and R. S. Azad, 1977: On turbulent entrainment at a stable density interface. *J. Fluid Mech.*, 79, 753-768.
- Lofquist, K., 1960: Flow and stress near an interface between stratified liquids. *Phys. Fluids*, 3, 158-175.
- Mahrt, L., and D. H. Lenschow, 1976: Growth dynamics of the convectively mixed-layer. *J. Atmos. Sci.*, 33, 41-51.
- Miller, J. R., 1976: The salinity effect in a mixed-layer ocean model. *J. Phys. Oceanogr.*, 6, 29-35.
- Moore, N. J., and R. R. Long, 1971: An experimental investigation of turbulent stratified shearing flow. *J. Fluid Mech.*, 49, 635-655.
- Niiler, P. P., and E. B. Kraus, 1977: One-dimensional models. *Modelling and Prediction of the Upper Layers of the Ocean*, E. B. Kraus, Ed., Pergamon Press, 285 pp.
- Ostapoff, F., Y. Tarbeyev and S. Worthem, 1973: Heat flux and precipitation estimates from oceanographic observations. *Science*, 180, 960-962.
- Price, J. F., 1978: Interpreting laboratory models of the mixed-layer. *Ocean Modelling*, 10, 7-9. Unpublished manuscript.
- , C. N. K. Mooers and J. C. Van Leer, 1978: Observation and simulation of storm-induced mixed-layer deepening. *J. Phys. Oceanogr.*, 8, 582-599.
- Thorpe, S. A., 1971: Experiments on the instability of stratified shear flows: miscible fluids. *J. Fluid Mech.*, 46, 299-320.
- , 1973: Turbulence in stably stratified fluids: a review of laboratory experiments. *Bound.-Layer Meteor.*, 5, 95-119.
- Turner, J. S., 1973: *Buoyancy Effects in Fluids*. Cambridge University Press, 367 pp.